IEEE Access
Multidisciplinary | Rapid Review | Open Access Journal

Received October 22, 2019, accepted November 2, 2019, date of publication November 5, 2019, date of current version November 15, 2019.

Digital Object Identifier 10.1109/ACCESS.2019.2951696

High-Gain Observer-Based Sliding Mode Force Control for the Single-Rod Electrohydraulic Servo Actuator

GUOSHENG XU, NIANLI LU, AND GUANGMING LV
School of Mechatronics Engineering, Harbin Institute of Technology, Harbin 150001, China
Corresponding author: Guosheng Xu (xgsh@hit.edu.cn)

ABSTRACT A high-gain observer based sliding mode force control system for the single-rod servo actuator is presented in this paper. In order to track the desired force, full states for feedback are needed. Since only the output force is measured, a high-gain observer with easy implementation and calibration is designed for the estimation of the unavailable states. Then the sliding mode controller is proposed and a continuously varying function instead of the traditional sign function is used to constitute the switching term of the control input which takes the distance of the system states from the sliding surface into account. So the chattering phenomena are eliminated. The stability of the closed-loop force control system is analyzed by the singular perturbation method and simulations show the effectiveness of the proposed force control method for the single-rod electrohydraulic servo actuator.

INDEX TERMS High-gain observer, sliding mode control, chattering-free, servo actuator, force control.

I. INTRODUCTION

For the high stiffness, rapid response, and the perfect capability to provide large driving forces or torques, electrohydraulic systems (EHS) are widely used in industrial equipment. The controlled forces or pressures with fast response and high accuracy are significantly required for the EHS applied in metal forming machines, injection moulding machines, hydraulic punching, riveting, pressing machines, industrial robots interacting with the environment, etc. Deticek and Kiker [1] designed an adaptive force controller of hydraulic drives of facility for testing mechanical constructions. Experimental results prove the effectiveness of the proposed new control algorithm consisting of the combination of a proportional integral differential (PID) controller and an adaptive feedforward velocity loop in the force control of the hydraulic drives and the steady error remains zero with the overshoot of the control variable less than 5% no matter what large the disturbance velocity is. Robertsson *et al.* [2] designed and implemented a platform for fast external sensor integration into an industrial robot system with easy reconfigurable control structure which was able to control contact forces with a sampling bandwidth of an order of magnitude higher than for conventional robot controllers. Chen *et al.* [3] proposed robust cascade force control strategy for 1-degree-of-freedom (1-DOF) hydraulically actuated exoskeleton. Simulations and experiments indicate that the proposed approach can achieve smaller human-machine interaction force and good robust performance to model uncertainties. Rossi *et al.* [4] presented an online estimation algorithm of environment stiffness in the force control for the industrial robot. The control approaches are experimentally validated on an industrial robot and proved to be robust to environment stiffness and joint friction disturbances. Based on the virtual decomposition control approach, Koivumaki and Mattila [5] introduced a high-performance controller for heavy-duty contact force control without engaging fragile force/torque sensors. According to the experiments, the proposed controller can achieve a force control accuracy of 4.1% at a desired contact force of 8000N which can be considered a significant result due to highly nonlinear behavior of the articulated hydraulic manipulator and the complex interaction dynamics between the manipulator and the environment. Adaptive robust backstepping control or self-tuning grey predictor combined with a fuzzy PID is suggested in the hydraulic load simulator force control system [6], [7]. Experiments show better tracking performance and higher control precision compared with conventional PID controller. By adding compliance through special hoses or springs, improved tracking performance of hydraulic actuator force control system is presented in [8]–[10].

The associate editor coordinating the review of this manuscript and approving it for publication was Mohsin Jamil.

Alleyne and Liu [11] showed the limitations of simple controllers used in the hydraulic servo-systems force tracking control and more advanced control algorithms were a necessity rather than a luxury. Thus, many advanced algorithms are developed in the force control of hydraulic actuator systems. Niksefat and Sepehri [12] designed a robust force controller via quantitative feedback theory (QFT). The experiments demonstrate the robustness of the QFT controller for up to 100% variations in environment stiffness, supply pressure and force setpoint. The feedforward neural network or feedforward compensator is employed in [13]–[15]. In order to improve the control quality, robust training mechanism or self-tuning algorithm is used. Jerouane *et al.* [16] introduced variable structure control (VSC) method for the hydraulic actuators force control. Three reaching laws are developed with the sliding mode equivalence law to further improve the force tracking performance. Xiao *et al.* [17] created a novel cascaded sliding mode controller (SMC). Simulations show the good tracking precision, fast convergence and smooth control input for the desired constant force control.

In the above hydraulic actuator force control systems, more than the force information is required to constitute the control term. So the displacement sensor, speed sensor, force sensor, and pressure transducer are used. Thus, there inevitably will be measurement error. Furthermore, the derivative of the measured signal is also needed and it may amplify the measurement noise and is not easy to be gotten. In order to reduce the number of sensors, observers for state estimation are applied. Based on the H_∞ performance, robust shaft torque observer is designed for the estimation of the torque which can not be easily measured by using affordable sensors in electric vehicle system [18], [19]. Simulations demonstrate the validation of the proposed observer design. Zhang and Wang designed a mode-dependent and fuzzy-basis-dependent Takagi–Sugeno fuzzy filter by using the transmitted packet subject to the described network issue [20]. The tunnel-diode circuit in a network environment is presented to show the effectiveness and the advantage of the proposed approach. Shi *et al.* [21] provided an extended-state-observer-based chattering free sliding mode controller for systems with matched and mismatched uncertainties and simulations showed the good performance of extended state observer in estimating the mismatched disturbance. High-gain sliding mode observer (SMO) and adaptive fuzzy SMO are used to estimate state and unknown parameters [22]–[24]. Experimental results demonstrate that the proposed observer has higher estimation precision than the traditional SMO. Sun and Chiu [25] used disturbance observer-based sliding mode controller to make the hydraulic actuator system track the desired force with uncertainty compensation. Since full states are required, high-gain observer (HO) with easier implementation and calibration compared with above complicated observers is suggested in the force controller design of the EHS considering the limitations imposed by cost and space. Nakkarat and Kuntanapreeda [26] designed a proportional integral observer-based backstepping controller (PIOBC) and the experimental results demonstrated higher efficiency compared with the industrial P or PI controllers. Observer based output feedback domination approach is applied to the force tracking of electrohydraulic actuators in [27]. The control scheme offers a better tracking performance than the conventional backstepping control method through numerical simulation results. Though the above observer-based hydraulic actuator force controllers show good performance, the convergence of the coupling of the observer and the force controllers is not theoretically confirmed.

Recently, a high-gain observer-based integral SMC of the EHS is designed to track the desired position in [28]. Results of simulations and experiments indicate that the controller can reduce the position tracking error and position ripples compared with the backstepping controller. And the entire system stability is proven using singular perturbation theorem. A passivity-based controller with HO is implemented for the position tracking of the EHS in [29], [30]. Simulations and experiments show the effectiveness of the proposed method and the stability of the closed-loop is also studied by singular perturbation theorem. Thus, by singular perturbation theory, the convergence of the coupling of the observer and the force controller for the EHS can be proved.

In this paper, a high-gain observer-based sliding mode force controller for the single-rod electrohydraulic servo actuator is constructed. Due to the simplicity in application and insensitivity to parameter changes and external disturbance, SMC is widely used in the position or force control of EHS [16], [17], [25], [28], [31], [32]. The rest of this paper is organized as follows. Section 2 presents the mathematical model of the electrohydraulic servo actuator. Section 3 provides the design of a HO with easy implementation and calibration and the chattering-free SMC in which a continuously varying function instead of the traditional sign function is used to constitute the switching term. The convergence proofs of the observer and the SMC are given respectively. Section 4 illustrates the stability analysis of the closed-loop electrohydraulic actuator force control system. Simulation results of the proposed method for the desired force tracking are given in Section 5 and section 6 draws a brief conclusion.

II. PROBLEM STATEMENT

The EHS used in this paper is shown in Fig. 1. It consists of an asymmetrical cylinder, a servo solenoid valve, a computer, an interface board and a force sensor. The EHS is consistent with that in [17], [26], and [27]. P_s is the supply pressure and P_r is the tank pressure. Q_1 and Q_2 are the oil flows of head-side and rod-side of the cylinder respectively. The hydraulic pressure and piston area for the head-side are represented by P_1 and A_1 as well as P_2 and A_2 for the rod-side. The load's force which is measured by the force sensor is applied to the end of the piston rod. And through the interface board, force signal is fed back to the computer. Control signal generated from the computer controller is converted by the interface board and transmitted to the servo solenoid valve.

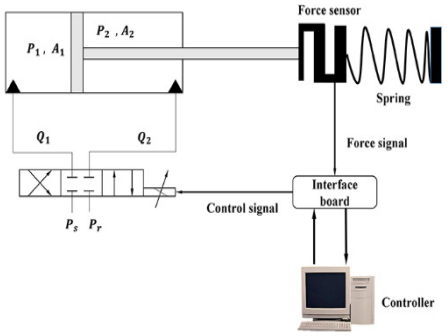

FIGURE 1. Schematic of EHS.

The load equation of the single-rod actuator system shown in Fig. 1 is [33], [34],

$$m\ddot{L} = P_1A_1 - P_2A_2 - c\dot{L} - F - F_f \tag{1}$$

where L is the actuator's displacement, F is the load's force and modelled as a pure spring with $F = k_sL$, k_s is the spring stiffness, F_f is the friction force and assumed can be ignored [17], [26]. m and c represent the mass of the moving part and the equivalent viscous damping coefficient respectively. The continuity equation for the flows through the cylinder neglecting all the leakage is [12],

$$\begin{cases} \dot{P}_1 = \dfrac{\beta_e}{V_1}(Q_1 - A_1\dot{L}) \\ \dot{P}_2 = \dfrac{\beta_e}{V_2}(A_2\dot{L} - Q_2) \end{cases} \tag{2}$$

where β_e is the effective bulk modulus of the hydraulic oil, $V_1 = V_{01} + A_1L$ and $V_2 = V_{02} - A_2L$ are the head-side and rod-side chamber volumes of the cylinder, V_{01} and V_{02} are the corresponding chamber volumes when $L = 0$. As the servovalve has a linear flow gain characteristic [35], the flows Q_1 and Q_2 can be linearly mapped on the input voltage V_{in} as follows:

$$\begin{cases} Q_1 = \begin{cases} \gamma KV_{in}, & \dot{L} < 0 \\ KV_{in}, & \dot{L} \geq 0 \end{cases} \\ Q_2 = \begin{cases} KV_{in}, & \dot{L} < 0 \\ \dfrac{K}{\gamma}V_{in}, & \dot{L} \geq 0 \end{cases} \end{cases} \tag{3}$$

where K is the flow/signal gain of the servovalve, $\gamma = A_1/A_2$ is the cylinder's flow factor.

Using the relationship $L = F/k_s$, $\dot{L} = \dot{F}/k_s$, and $\ddot{L} = \ddot{F}/k_s$, the complete dynamic model of the EHS in Fig. 1 can be written as [17], [26]:

$$\begin{cases} \dot{x}_1 = x_2 \\ \dot{x}_2 = -\dfrac{k_s}{m}x_1 - \dfrac{c}{m}x_2 + \dfrac{k_s}{m}x_3 \\ \dot{x}_3 = -\mathrm{g}_1(x_1)\,x_2 + \mathrm{g}_2(x_1)\,u \end{cases} \tag{4}$$

$$y = \bar{C}x = x_1 \tag{5}$$

where

$$\mathrm{g}_1(x_1) = \frac{\beta_eA_1^2}{k_sV_{01} + A_1x_1} + \frac{\beta_eA_2^2}{k_sV_{02} - A_2x_1}$$

$$\mathrm{g}_2(x_1) = \frac{\beta_eA_1Kk_s}{k_sV_{01} + A_1x_1} + \frac{\beta_eA_2Kk_s}{(k_sV_{02} - A_2x_1)\,\gamma}$$

$$u = \begin{cases} \gamma V_{in}, & \dot{x}_1 < 0 \\ V_{in}, & \dot{x}_1 \geq 0 \end{cases}$$

x_1, x_2, and x_3 represent the force F, the derivative of the force $\dot{F}$, and the hydraulic driving force $P_1A_1 - P_2A_2$ respectively. $x = \begin{bmatrix} x_1 & x_2 & x_3 \end{bmatrix}^T$, $\bar{C} = [\,1 \;\; 0 \;\; 0\,]$, and u is defined as the system input.

III. CONTROLLER DESIGN

A. HIGH-GAIN OBSERVER DESIGN

In order to utilize SMC, full-state information is needed. Since only x_1 (force) is available, a HO with easy implementation and calibration is designed to estimate the unmeasured states. The observer is given by the following equation [36]–[39]:

$$\dot{\hat{x}} = f(u, \hat{x}) - \frac{1}{\varepsilon}\Lambda^+(u, x)\,\Delta_\varepsilon^{-1}P^{-1}C^T\bar{C}(\hat{x} - x) \tag{6}$$

where $\hat{x} = \begin{bmatrix} \hat{x}_1 & \hat{x}_2 & \hat{x}_3 \end{bmatrix}^T$ is the observer's estimation states and

$$f(u, \hat{x}) = \begin{bmatrix} f_1(u, \hat{x}) \\ f_2(u, \hat{x}) \\ f_3(u, \hat{x}) \end{bmatrix} = \begin{bmatrix} \hat{x}_2 \\ -\dfrac{k_s}{m}\hat{x}_1 - \dfrac{c}{m}\hat{x}_2 + \dfrac{k_s}{m}\hat{x}_3 \\ -\mathrm{g}_1(\hat{x}_1)\,\hat{x}_2 + \mathrm{g}_2(\hat{x}_1)\,u \end{bmatrix}$$

$$\Lambda(u, x) = \mathrm{diag}\left[1, \frac{\partial f_1}{\partial x_2}(u, \hat{x}), \frac{\partial f_1}{\partial x_2}(u, \hat{x})\frac{\partial f_2}{\partial x_3}(u, \hat{x})\right] = \mathrm{diag}\left[1, 1, \frac{k_s}{m}\right]$$

$\Lambda^+(u, x)$ is the left inverse of the matrix $\Lambda(u, x)$; $\Delta_\varepsilon = \mathrm{diag}[1, \varepsilon, \varepsilon^2]$ and ε is a small positive constant; P is the unique solution of the algebraic Lyapunov equation

$$P + A^TP + PA - C^TC = 0 \tag{7}$$

where $P^{-1}C^T = \begin{bmatrix} C_3^1 & C_3^2 & C_3^3 \end{bmatrix}^T = [\,3 \;\; 3 \;\; 1\,]^T$ with $C_n^p = \frac{n!}{(n-p)!p!}$;

$$A = \begin{bmatrix} 0 & 1 & 0 \\ 0 & 0 & 1 \\ 0 & 0 & 0 \end{bmatrix}, \quad C = [\,1 \quad 0 \quad 0\,].$$

Then the high-gain observer based on (6) for the electrohydraulic actuator is as follows:

$$\begin{cases} \dot{\hat{x}}_1 = \hat{x}_2 + \dfrac{3}{\varepsilon}(y - \hat{x}_1) \\ \dot{\hat{x}}_2 = -\dfrac{k_s}{m}\hat{x}_1 - \dfrac{c}{m}\hat{x}_2 + \dfrac{k_s}{m}\hat{x}_3 + \dfrac{3}{\varepsilon^2}(y - \hat{x}_1) \\ \dot{\hat{x}}_3 = -\mathrm{g}_1(\hat{x}_1)\,\hat{x}_2 + \mathrm{g}_2(\hat{x}_1)\,u + \dfrac{m}{k_s\varepsilon^3}(y - \hat{x}_1) \end{cases} \tag{8}$$

According to Farza *et al.* [36], [37], the HO used in this paper is globally and exponentially stable and $\exists\varepsilon_0 > 0$; $\forall\varepsilon < \varepsilon_0$; $\exists\lambda > 0$; $\exists\mu_\varepsilon > 0$; $\exists M_\varepsilon > 0$; $\forall u \in U$; $\forall\hat{x}(0) \in R^3$, the estimation error

$$\left\|\hat{x}(t) - x(t)\right\| \leq \lambda\frac{1}{\varepsilon^2}e^{-\mu_\varepsilon t}\left\|\hat{x}(0) - x(0)\right\| + M_\varepsilon\sigma \quad (9)$$

where σ is the upper bound of the system uncertainties. Besides, $\lim_{\varepsilon\to 0}\mu_\varepsilon = +\infty$ and $\lim_{\varepsilon\to 0}M_\varepsilon = 0$. So the convergence rate of the estimation error can be adjusted through a proper choice of the observer bandwidth parameter ε.

B. SLIDING MODE CONTROLLER DESIGN

To design the SMC, new state variables are defined as:

$$\begin{cases} z_1 = x_1 \\ z_2 = x_2 \\ z_3 = -\dfrac{k_s}{m}x_1 - \dfrac{c}{m}x_2 + \dfrac{k_s}{m}x_3 \end{cases} \quad (10)$$

Then the original system (4), (5) are transformed as:

$$\begin{cases} \dot{z}_1 = z_2 \\ \dot{z}_2 = z_3 \\ \dot{z}_3 = -\left(\dfrac{k_s}{m} + \dfrac{k_s}{m}\mathrm{g}_1(z_1)\right)z_2 - \dfrac{c}{m}z_3 + \dfrac{k_s}{m}\mathrm{g}_2(z_1)u \end{cases} \quad (11)$$

$$y = \bar{C}z = z_1 \quad (12)$$

where $z = \begin{bmatrix} z_1 & z_2 & z_3 \end{bmatrix}^T$, $\mathrm{g}_1(z_1) = \mathrm{g}_1(x_1)$, and $\mathrm{g}_2(z_1) = \mathrm{g}_2(x_1)$.

Define the sliding surface s as:

$$s = a^2e_1 + 2ae_2 + e_3 \quad (13)$$

where $e = \begin{bmatrix} e_1 & e_2 & e_3 \end{bmatrix}^T$ is the tracking error, $e_1 = y_d - z_1$, $e_2 = \dot{y}_d - z_2$ and $e_3 = \ddot{y}_d - z_3$. a is a positive constant and y_d represents the desired tracking force. Differentiating (13), the following equation is obtained:

$$\begin{aligned} \dot{s} &= a^2e_2 + 2ae_3 + \dot{e}_3 \\ &= a^2e_2 + 2ae_3 + \dddot{y}_d + \left(\frac{k_s}{m} + \frac{k_s}{m}\mathrm{g}_1(z_1)\right)z_2 \\ &\quad + \frac{c}{m}z_3 - \frac{k_s}{m}\mathrm{g}_2(z_1)u \end{aligned} \quad (14)$$

Based on the feedback sliding mode control, the control input is,

$$u = u_{eq} + u_{sw} \quad (15)$$

where

$$\begin{aligned} u_{eq} &= \frac{m}{k_s\mathrm{g}_2(z_1)}\left[a^2e_2 + 2ae_3 + \dddot{y}_d \right. \\ &\quad \left. + \left(\frac{k_s}{m} + \frac{k_s}{m}\mathrm{g}_1(z_1)\right)z_2 + \frac{c}{m}z_3\right] \\ u_{sw} &= \frac{m}{k_s\mathrm{g}_2(z_1)}\Gamma\mathrm{sign}(s) \end{aligned}$$

u_{eq} is the equivalent control term given by $\dot{s} = 0$, u_{sw} is the switching control term given by the reaching condition $s\dot{s} \leq 0$, and Γ is positive constant. To attenuate and eliminate the chattering phenomena, the switching control term u_{sw} is replaced by

$$u_{sw} = \frac{m}{k_s\mathrm{g}_2(z_1)}\Gamma s \quad (16)$$

The proposed control law (16) takes the distance of the state from the sliding surface into account and uses smooth and continuous function instead of sign function [40]. To analyze the control stability, a Lyapunov candidate function is defined as:

$$V = \frac{1}{2}s^2 \quad (17)$$

Then derivative of V is,

$$\begin{aligned} \dot{V} &= s\dot{s} = s\left(a^2e_2 + 2ae_3 + \dddot{y}_d - \dot{z}_3\right) \\ &= s\left(a^2e_2 + 2ae_3 + \dddot{y}_d + \left(\frac{k_s}{m} + \frac{k_s}{m}\mathrm{g}_1(z_1)\right)z_2 \right. \\ &\quad \left. + \frac{c}{m}z_3 - \frac{k_s}{m}\mathrm{g}_2(z_1)u\right) \\ &= -\Gamma s^2 = -2\Gamma V \leq 0 \end{aligned} \quad (18)$$

Thus, the control system is asymptotically stable and V exponentially converges to zero. And $V \to 0 \Rightarrow s \to 0$,

$$\begin{bmatrix} \dot{e}_1 \\ \dot{e}_2 \end{bmatrix} = \underbrace{\begin{bmatrix} 0 & 1 \\ -a^2 & -2a \end{bmatrix}}_{A_e}\begin{bmatrix} e_1 \\ e_2 \end{bmatrix} \quad (19)$$

since A_e is Hurwitz, the tracking error e also exponentially converges to zero.

IV. CLOSED-LOOP STABILITY ANALYSIS

Define the state estimation error $\tilde{x}$ and the scaled estimation error η as:

$$\begin{cases} \tilde{x} = x - \hat{x} = \begin{bmatrix} \tilde{x}_1 \\ \tilde{x}_2 \\ \tilde{x}_3 \end{bmatrix} = \begin{bmatrix} x_1 - \hat{x}_1 \\ x_2 - \hat{x}_2 \\ x_3 - \hat{x}_3 \end{bmatrix} \\ \eta = \begin{bmatrix} \eta_1 \\ \eta_2 \\ \eta_3 \end{bmatrix} = \begin{bmatrix} \dfrac{1}{\varepsilon^2}\tilde{x}_1 \\ \dfrac{1}{\varepsilon}\tilde{x}_2 \\ \tilde{x}_3 \end{bmatrix} \end{cases} \quad (20)$$

Then the dynamics of the scaled estimation error η can be written as a fast dynamics in a singularly perturbed form

$$\varepsilon\dot{\eta} = A\eta + \varepsilon\delta(\eta, x, \hat{x}, u) \quad (21)$$

where

$$A = \begin{bmatrix} A_1 \\ A_2 \\ A_3 \end{bmatrix} = \begin{bmatrix} -3 & 1 & 0 \\ -3 & 0 & \dfrac{k_s}{m} \\ -\dfrac{m}{k_s} & 0 & 0 \end{bmatrix}$$

$$\delta\left(\eta, x, \hat{x}, u\right) = \begin{bmatrix} \delta_1 \\ \delta_2 \\ \delta_3 \end{bmatrix} = \begin{bmatrix} 0 \\ -\frac{k_s}{m}\varepsilon\eta_1 - \frac{c}{m}\eta_2 \\ \mathrm{g}_1\left(\hat{x}_1\right)\hat{x}_2 - \mathrm{g}_1\left(x_1\right)x_2 + \left(\mathrm{g}_2\left(x_1\right) - \mathrm{g}_2\left(\hat{x}_1\right)\right)u \end{bmatrix}$$

As only z_1 (force) is available for measurement, the control input u uses $\hat{x}$ instead of x in the SMC. Thus the control law (15) becomes

$$u = \frac{m}{k_s \mathrm{g}_2\left(\hat{z}_1\right)}\left[a^2\hat{e}_2 + 2a\hat{e}_3 + \dddot{y}_d + \left(\frac{k_s}{m} + \frac{k_s}{m}\mathrm{g}_1\left(\hat{z}_1\right)\right)\hat{z}_2 + \frac{c}{m}\hat{z}_3 + \Gamma\hat{s}\right] \quad (22)$$

where $\hat{e}_1 = y_d - \hat{z}_1$, $\hat{e}_2 = \dot{y}_d - \hat{z}_2$, $\hat{e}_3 = \ddot{y}_d - \hat{z}_3$, $\hat{z}_i\, i \in [1, 2]$, $\dot{\hat{z}}_3 = -\frac{k_s}{m}\hat{x}_1 - \frac{c}{m}\hat{x}_2 + \frac{k_s}{m}\hat{x}_3$, $\hat{s} = a^2\hat{e}_1 + 2a\hat{e}_2 + \hat{e}_3$, $\tilde{s} = s - \hat{s} = \left(\frac{k_s}{m} - a^2\right)\tilde{x}_1 + \left(\frac{c}{m} - 2a\right)\tilde{x}_2 - \frac{k_s}{m}\tilde{x}_3$, and $\dot{\tilde{s}} = \left[\left(\frac{k_s}{m} - a^2\right)\varepsilon \quad \left(\frac{c}{m} - 2a\right) \quad -\frac{k_s}{m\varepsilon}\right]\varepsilon\dot{\eta}$. Thus the derivative of the sliding surface s is,

$$\begin{aligned}\dot{s} &= \dddot{s} + \dot{\hat{s}} = \dddot{s} + a^2\hat{e}_2 + 2a\hat{e}_3 + \dddot{y}_d \\ &\quad + \left(\frac{k_s}{m} + \frac{k_s}{m}\mathrm{g}_1\left(\hat{z}_1\right)\right)\hat{z}_2 + \frac{c}{m}\hat{z}_3 - \frac{k_s}{m}\mathrm{g}_2\left(\hat{z}_1\right)u \\ &= \dddot{s} - \Gamma\hat{s} = -\Gamma s + \dddot{s} + \Gamma\tilde{s} = -\Gamma s + f\left(\tilde{s}\right) \end{aligned} \quad (23)$$

where $f\left(\tilde{s}\right) = \dddot{s} + \Gamma\tilde{s}$.

The closed-loop force control system can be represented in the standard singularly perturbed form as follows:

$$\begin{cases} \varepsilon\dot{\eta} = A\eta + \varepsilon\delta(\eta, x, \hat{x}, u) \\ \dot{s} = -\Gamma s + f\left(\tilde{s}\right) \end{cases} \quad (24)$$

with the equilibrium point $(s, \eta) = (0, 0)$. s is the slow state, η is the fast state. Since A is Hurwitz, making $\varepsilon = 0$ implies that $\eta_i = 0$, $x_i = \hat{x}_i$, $\tilde{x}_i = 0\, i \in [1, 2, 3]$, $\dot{\tilde{s}} = \tilde{s} = f\left(\tilde{s}\right) = 0$. And leaving the quasi-steady-state model of the slow dynamics as,

$$\dot{s} = -\Gamma s \quad (25)$$

According to the design of the feedback SMC, s exponentially converges to zero. Transforming the slow time-scale t to the fast time-scale $\tau = t/\varepsilon$, system (24) becomes,

$$\begin{cases} \frac{d}{d\tau}\eta = A\eta + \varepsilon\delta\left(\eta, x, \hat{x}, u\right) \\ \frac{d}{d\tau}s = -\varepsilon\Gamma s + \varepsilon f\left(\tilde{s}\right) \end{cases} \quad (26)$$

as $\varepsilon \longrightarrow 0$, it yields the boundary layer system

$$\frac{d}{d\tau}\eta = A\eta \quad (27)$$

since A is Hurwitz, a positive definite matrix P_η exists such that

$$A^T P_\eta + P_\eta A = -I \quad (28)$$

define a Lyapunov candidate function as:

$$V_\eta = \eta^T P_\eta \eta \quad (29)$$

Then the derivative of V_η to the fast time-scale τ is,

$$\frac{d}{d\tau}V_\eta = \eta^T\left(A^T P_\eta + P_\eta A\right)\eta = -\eta^T\eta \leq 0 \quad (30)$$

so $\eta = 0$ is asymptotically stable. According to the system (24), η is much faster than s, then $\eta = 0 \rightarrow x = \hat{x}, \tilde{x} = f\left(\tilde{s}\right) = 0 \rightarrow s = 0$, and the tracking error e decays exponentially. In practice, $\varepsilon = 0$ can't be achieved for the observer [30]. From (9), $\exists\varepsilon_0 > 0$; $\forall\varepsilon < \varepsilon_0$; $\lim_{t\to+\infty}\hat{x} = x$ and $\lim_{t\to+\infty}\eta = 0$. And by reducing the value of ε, the state estimates $\tilde{x}(\eta)$ vary quickly and are capable of tracking the abrupt state variations. However, too small ε will make the observer become noise sensitive, then the value of ε is a compromise between a good tracking performance of the state variations and a satisfactory behaviour with noise rejection [36], [41]–[43].

V. SIMULATIONS

A. SYSTEM WITHOUT UNCERTAINTIES

The parameters in [26] are used for simulation to demonstrate the efficiency of the proposed high-gain observer-based sliding mode controller (HOSMC). $\beta_e = 1.5 \times 10^9\mathrm{N/m^2}$, $K = 3.7 \times 10^{-6}\mathrm{m^3/V}$, $A_1 = 2.463 \times 10^{-3}\mathrm{m^2}$, $A_2 = 1.455 \times 10^{-3}\mathrm{m^2}$, $V_{01} = 3.079 \times 10^{-4}\mathrm{m^3}$, $V_{02} = 1.820 \times 10^{-4}\mathrm{m^3}$, $m = 6.0\mathrm{kg}$, $c = 500\mathrm{N/ms^{-1}}$, $k_s = 1.206 \times 10^5\mathrm{N/m}$ and $\gamma = A_1/A_2$. The design parameters of the HOSMC are chosen as $\varepsilon = 0.01$, $a = 10$, and $\Gamma = 1000$. The initial states of the EHS (4) and the high-gain observer (8) are set as $x = \hat{x} = \begin{bmatrix} 0 & 0 & 0 \end{bmatrix}^T$. For comparison, the proportional integral observer (PIO) and the PIOBC in [26] is also employed. Parameters of the PIO are $L_1 = \begin{bmatrix} 0.181 & 0.016 & 0.104 \end{bmatrix}^T$ and $L_2 = \begin{bmatrix} 0 & 0 & 10000 \end{bmatrix}^T$. Parameters of the backstepping controller are $k_1 = 1.5$, $k_2 = 1.0$, and $k_3 = 1.0$.

Fig. 2 shows the reference sinusoidal force signal $r\,(t) = 1200 + 200\sin(2t)$ estimation error by HO and PIO respectively. Fig. 3 and Fig. 6 are the curves of the reference

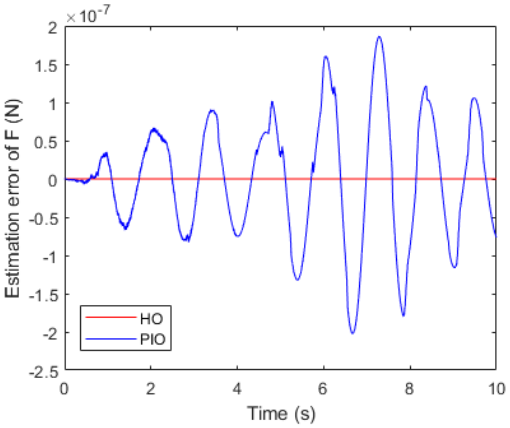

FIGURE 2. Comparison of observer's estimation error of F: $r\,(t) = 1200 + 200\sin(2t)$.

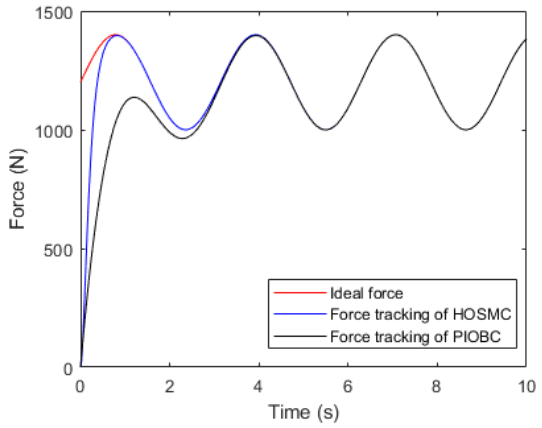

FIGURE 3. Comparison of sinusoidal responses: $r(t) = 1200 + 200\sin(2t)$.

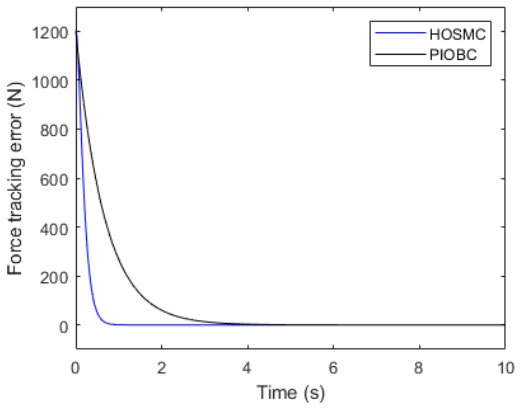

FIGURE 4. Comparison of force tracking error: $r(t) = 1200 + 200\sin(2t)$.

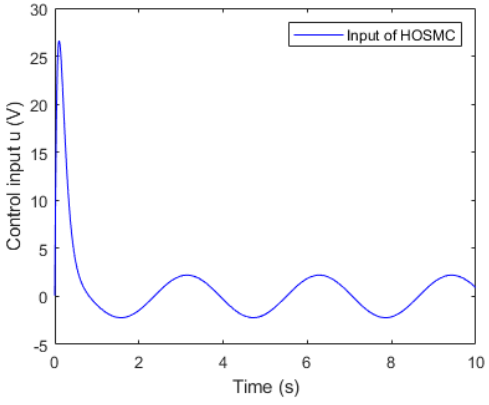

FIGURE 5. Force control input: $r(t) = 1200 + 200\sin(2t)$.

sinusoidal force tracking performance by HOSMC and PIOBC. Fig. 4 and Fig. 5 present the force tracking error and the control input u of the reference sinusoidal force signal $r(t) = 1200 + 200\sin(2t)$.

Without noise and other friction, the proposed HO shows higher estimation precision than the PIO from Fig. 2 and the proposed HOSMC tracks the variable reference force signal with faster response and quicker convergence than the PIOBC

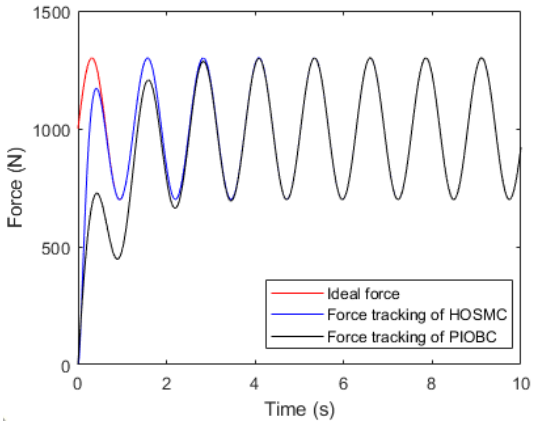

FIGURE 6. Comparison of sinusoidal responses: $r(t) = 1000 + 300\sin(5t)$.

from Fig. 3, Fig. 4 and Fig. 6. From Fig. 5, the control input is smooth with no chattering. Therefore, the proposed HOSMC is significant and effective in the force control of the single-rod EHS.

B. SYSTEM WITH UNCERTAINTIES

Consider the EHS in the presence of the matched and mismatched uncertainties or disturbances as follows:

$$\begin{cases} \dot{x}_1 = x_2 \\ \dot{x}_2 = -\dfrac{k_s}{m}x_1 - \dfrac{c}{m}x_2 + \dfrac{k_s}{m}x_3 + d_1(t) \\ \dot{x}_3 = -\mathrm{g}_1(x_1)\,x_2 + \mathrm{g}_2(x_1)\,u_q + d_2(t) \end{cases} \tag{31}$$

where $d_1(t)$ is the mismatched uncertainties and appears in a different channel from the control input u_q, $d_2(t)$ is the matched uncertainties [21]. $d_1(t)$ is differentiable and is bounded. New state variables $q = \begin{bmatrix} q_1 & q_2 & q_3 \end{bmatrix}^T$ are defined as:

$$\begin{cases} q_1 = x_1 \\ q_2 = x_2 \\ q_3 = -\dfrac{k_s}{m}x_1 - \dfrac{c}{m}x_2 + \dfrac{k_s}{m}x_3 + d_1(t) \end{cases} \tag{32}$$

Then system (31) becomes,

$$\begin{cases} \dot{q}_1 = q_2 \\ \dot{q}_2 = q_3 \\ \dot{q}_3 = -\left(\dfrac{k_s}{m} + \dfrac{k_s}{m}\mathrm{g}_1(q_1)\right) q_2 - \dfrac{c}{m}q_3 + \dfrac{k_s}{m}\mathrm{g}_2(q_1)\,u_q \\ \quad + d(t) \end{cases} \tag{33}$$

where $d(t) = \frac{k_s}{m}d_2(t) + \dot{d}_1(t)$ and $|d(t)| \leq \sigma$. Unlike observer design (8) for the initial system (4), the high-gain observer in the presence of uncertainties should be built for the transformed system (33) in order to compensate the mismatched uncertainties existing in system (31). Thus, the HO

$\hat{q} = \left[\hat{q}_1 \;\; \hat{q}_2 \;\; \hat{q}_3\right]^T$ based on (6) for system (33) is,

$$\begin{cases} \dot{\hat{q}}_1 = \hat{q}_2 + \dfrac{3}{\varepsilon}\left(y - \hat{q}_1\right) \\ \dot{\hat{q}}_2 = \hat{q}_3 + \dfrac{3}{\varepsilon^2}\left(y - \hat{q}_1\right) \\ \dot{\hat{q}}_3 = -\left(\dfrac{k_s}{m} + \dfrac{k_s}{m}\mathrm{g}_1\left(\hat{q}_1\right)\right)\hat{q}_2 - \dfrac{c}{m}\hat{q}_3 + \dfrac{k_s}{m}\mathrm{g}_2\left(\hat{q}_1\right)u_q \\ \quad + \dfrac{1}{\varepsilon^3}\left(y - \hat{q}_1\right) \end{cases} \tag{34}$$

where $y = \bar{C}q = q_1 = x_1$. Define $e_q = \left[e_{q1} \;\; e_{q2} \;\; e_{q3}\right]^T = \left[y_d - q_1 \;\; \dot{y}_d - q_2 \;\; \ddot{y}_d - q_3\right]^T$, $\hat{e}_q = \left[\hat{e}_{q1} \;\; \hat{e}_{q2} \;\; \hat{e}_{q3}\right]^T = \left[y_d - \hat{q}_1 \;\; \dot{y}_d - \hat{q}_2 \;\; \ddot{y}_d - \hat{q}_3\right]^T$, $s_q = a^2 e_{q1} + 2ae_{q2} + e_{q3}$, $\hat{s}_q = a^2\hat{e}_{q1} + 2a\hat{e}_{q2} + \hat{e}_{q3}$. According to (9), in the case where uncertainties are present but bounded by σ, the asymptotic estimation error $\left\|\hat{q} - q\right\|$ can be made as small as desired by choosing values of ε small enough [36], [37]. Then the derivative of the sliding surface $\hat{s}_q$ is,

$$\begin{aligned} \dot{\hat{s}}_q &= a^2\hat{e}_{q2} + 2a\hat{e}_{q3} + \dddot{y}_d - \dddot{\hat{q}}_3 = a^2\hat{e}_{q2} + 2a\hat{e}_{q3} \\ &\quad + \dddot{y}_d + \left(\frac{k_s}{m} + \frac{k_s}{m}\mathrm{g}_1\left(\hat{q}_1\right)\right)\hat{q}_2 + \frac{c}{m}\hat{q}_3 - \frac{k_s}{m}\mathrm{g}_2\left(\hat{q}_1\right)u_q \end{aligned} \tag{35}$$

By $\dot{\hat{s}}_q = 0$, the equivalent control law u_{qeq} is,

$$\begin{aligned} u_{qeq} = \frac{m}{k_s\mathrm{g}_2\left(\hat{q}_1\right)}\Bigg[&a^2\hat{e}_{q2} + 2a\hat{e}_{q3} + \dddot{y}_d \\ &+ \left(\frac{k_s}{m} + \frac{k_s}{m}\mathrm{g}_1\left(\hat{q}_1\right)\right)\hat{q}_2 + \frac{c}{m}\hat{q}_3\Bigg] \end{aligned} \tag{36}$$

Define the switch control law $u_{qsw} = \frac{m}{k_s\mathrm{g}_2(\hat{q}_1)}\Gamma\hat{s}_q$ to satisfy the reaching condition $\hat{s}_q\dot{\hat{s}}_q \le 0$, the total control input u_q for system (33) is,

$$\begin{aligned} u_q = \frac{m}{k_s\mathrm{g}_2\left(\hat{q}_1\right)}\Bigg[&a^2\hat{e}_{q2} + 2a\hat{e}_{q3} + \dddot{y}_d \\ &+ \left(\frac{k_s}{m} + \frac{k_s}{m}\mathrm{g}_1\left(\hat{q}_1\right)\right)\hat{q}_2 + \frac{c}{m}\hat{q}_3 + \Gamma\hat{s}\Bigg] \end{aligned} \tag{37}$$

The state estimation error $\tilde{q}$ and the scaled estimation error η_q are defined as:

$$\begin{cases} \tilde{q} = q - \hat{q} = \begin{bmatrix}\tilde{q}_1 \\ \tilde{q}_2 \\ \tilde{q}_3\end{bmatrix} = \begin{bmatrix}q_1 - \hat{q}_1 \\ q_2 - \hat{q}_2 \\ q_3 - \hat{q}_3\end{bmatrix} \\ \eta_q = \begin{bmatrix}\eta_{q1} \\ \eta_{q2} \\ \eta_{q3}\end{bmatrix} = \begin{bmatrix}\dfrac{1}{\varepsilon^2}\tilde{q}_1 \\ \dfrac{1}{\varepsilon}\tilde{q}_2 \\ \tilde{q}_3\end{bmatrix} \end{cases} \tag{38}$$

Then the dynamics of the scaled estimation error η_q in a singularly perturbed form is,

$$\varepsilon\dot{\eta}_q = A_q\eta_q + \varepsilon\delta\left(\eta_q, q, \hat{q}, u\right) \tag{39}$$

where

$$A_q = \begin{bmatrix}A_{q1} \\ A_{q2} \\ A_{q3}\end{bmatrix} = \begin{bmatrix}-3 & 1 & 0 \\ -3 & 0 & 1 \\ -1 & 0 & 0\end{bmatrix}$$

$$\begin{aligned} &\delta\left(\eta_q, q, \hat{q}, u\right) \\ &= \begin{bmatrix}\delta_{q1} \\ \delta_{q2} \\ \delta_{q3}\end{bmatrix} \\ &= \begin{bmatrix} 0 \\ 0 \\ -\dfrac{k_s\varepsilon}{m}\eta_{q2} + \dfrac{k_s}{m}\mathrm{g}_1\left(\hat{q}_1\right)\hat{q}_2 - \dfrac{k_s}{m}\mathrm{g}_1\left(q_1\right)q_2 - \dfrac{c}{m}\eta_{q3} \\ \quad + \dfrac{k_s}{m}\left(\mathrm{g}_2\left(q_1\right) - \mathrm{g}_2\left(\hat{q}_1\right)\right)u_q + d\left(t\right) \end{bmatrix} \end{aligned}$$

since $\tilde{s}_q = s_q - \hat{s}_q = -a^2\tilde{q}_1 - 2a\tilde{q}_2 - \tilde{q}_3$ and $\dot{\tilde{s}}_q = \left[-a^2\varepsilon \;\; -2a \;\; -\frac{1}{\varepsilon}\right]\varepsilon\dot{\eta}_q$, the derivative of the sliding surface s_q is,

$$\begin{aligned} \dot{s}_q &= \dot{\tilde{s}}_q + \dot{\hat{s}}_q = \dot{\tilde{s}}_q + a^2\hat{e}_{q2} + 2a\hat{e}_{q3} + \dddot{y}_d \\ &\quad + \left(\frac{k_s}{m} + \frac{k_s}{m}\mathrm{g}_1\left(\hat{q}_1\right)\right)\hat{q}_2 + \frac{c}{m}\hat{q}_3 - \frac{k_s}{m}\mathrm{g}_2\left(\hat{q}_1\right)u_q \\ &= \dot{\tilde{s}}_q - \Gamma\hat{s}_q = -\Gamma s_q + \dot{\tilde{s}}_q + \Gamma\tilde{s}_q \\ &= -\Gamma s_q + f\left(\tilde{s}_q\right) \end{aligned} \tag{40}$$

where $f\left(\tilde{s}_q\right) = \dot{\tilde{s}}_q + \Gamma\tilde{s}_q$. Then the entire observer-based SMC system can be written as:

$$\begin{cases} \varepsilon\dot{\eta}_q = A_q\eta_q + \varepsilon\delta(\eta_q, q, \hat{q}, u) \\ \dot{s}_q = -\Gamma s_q + f\left(\tilde{s}_q\right) \end{cases} \tag{41}$$

since A_q is Hurwitz and Γ is positive constant, the stability of the closed-loop can be analyzed the same as (24). Too small ε is avoided in practice since the estimator may become noise sensitive. Thus, the value of ε, the same as that in (8) is also a compromise between fast convergence and sensitivity to noise [36], [41]–[43]. To demonstrate the effectiveness of the controller, uncertainties are defined as $d_1\left(t\right) = 10\cos(t)$ and $d_2\left(t\right) = 100\cos(t)$. Fig. 7 is the force estimation error of the EHS with uncertainties by HO. Fig. 8 and Fig. 9 are the reference force signal tracking performance for the system (31).

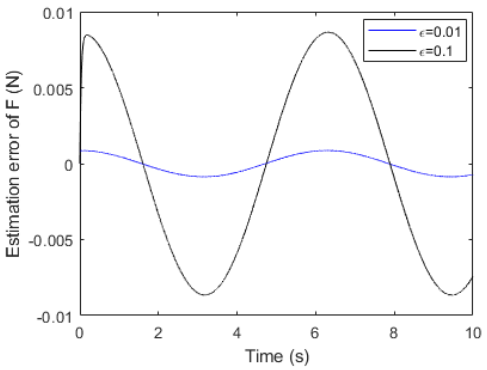

FIGURE 7. Observer's estimation error with $\Gamma = 1000$: $r\left(t\right) = 1200 + 200\sin(2t)$.

From Fig. 7, smaller ε improves the force estimation precision and can reduce the impact imposed by the matched or mismatched disturbance and uncertainties in the EHS. From Fig. 8 and Fig. 9, it can be seen that Γ governs

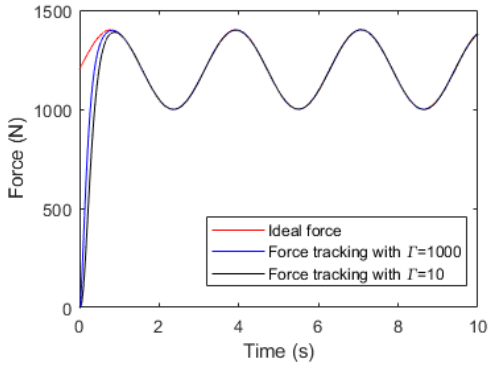

FIGURE 8. Sinusoidal responses with $\varepsilon = 0.01$: $r(t) = 1200 + 200\sin(2t)$.

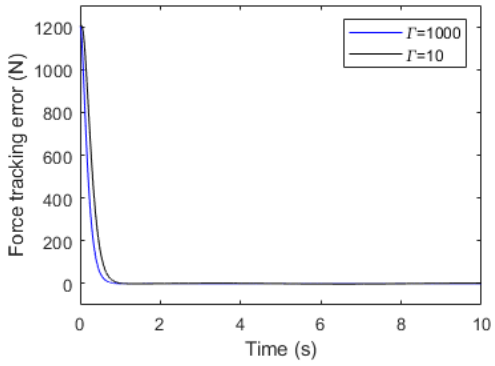

FIGURE 9. Force tracking error with $\varepsilon = 0.01$: $r(t) = 1200 + 200\sin(2t)$.

the controller convergence rate. Larger Γ makes controller system respond faster and converge more quickly.

VI. CONCLUSION

This paper presents a high-gain observer based sliding mode force control system for the single-rod EH servo actuator. Since only the force is available, a high-gain observer with easy implementation and calibration is designed to estimate the unmeasured states for feedback. And only the observer bandwidth parameter ε is adjusted. Then the SMC with chattering-free is proposed. The proof of the convergence of the closed-loop force tracking error is given by singular perturbation method. Simulation results show the superior tracking performance of the HOSMC with fast response, high tracking precision, and chattering-free in the force control of the single-rod EHS.

REFERENCES

[1] E. Detiček and E. Kiker, "An adaptive force control of hydraulic drives of facility for testing mechanical constructions," *Exp. Tech.*, vol. 25, no. 1, pp. 35–39, 2001.
[2] A. Robertsson, T. Olsson, R. Johansson, A. Blomdell, K. Nilsson, M. Haage, B. Lauwers, H. De Baerdemaeker, T. Brogardh, and H. Brantmark, "Implementation of industrial robot force control case study: High power stub grinding and deburring," in *Proc. IEEE Int. Conf. Intell. Robots Syst.*, Beijing, China, Oct. 2006, pp. 2743–2748.
[3] S. Chen, Z. Chen, B. Yao, X. Zhu, S. Zhu, Q. Wang, and Y. Song, "Adaptive robust cascade force control of 1-DOF hydraulic exoskeleton for human performance augmentation," *IEEE/ASME Trans. Mechatronics*, vol. 22, no. 2, pp. 589–600, Apr. 2017.
[4] R. Rossi, L. Fossali, A. Novazzi, L. Bascetta, and P. Rocco, "Implicit force control for an industrial robot based on stiffness estimation and compensation during motion," in *Proc. IEEE Int. Conf. Robot. Automat.*, Stockholm, Sweden, May 2016, pp. 1138–1145.
[5] J. Koivumäki and J. Mattila, "Stability-guaranteed force-sensorless contact force/motion control of heavy-duty hydraulic manipulators," *IEEE Trans. Robot.*, vol. 31, no. 4, pp. 918–935, Aug. 2015.
[6] J. Yao, Z. Jiao, and B. Yao, "Nonlinear adaptive robust backstepping force control of hydraulic load simulator: Theory and experiments," *J. Mech. Sci. Technol.*, vol. 28, no. 4, pp. 1499–1507, 2014.
[7] D. Q. Truong and K. K. Ahn, "Force control for hydraulic load simulator using self-tuning grey predictor—Fuzzy PID," *Mechatronics*, vol. 19, no. 2, pp. 233–246, 2009.
[8] J. A. L. Perez, E. R. De Pieri, and V. J. De Negri, "Force control of hydraulic actuators using additional hydraulic compliance," *Strojniski Vestnik/J. Mech. Eng.*, vol. 64, no. 10, pp. 579–589, 2018.
[9] M. V. Sivaselvan, A. M. Reinhorn, X. Shao, and S. Weinreber, "Dynamic force control with hydraulic actuators using added compliance and displacement compensation," *Earthquake Eng. Struct. Dyn.*, vol. 37, no. 15, pp. 1785–1800, 2008.
[10] Y. Chae, R. Rabiee, A. Dursun, and C.-Y. Kim, "Real-time force control for servo-hydraulic actuator systems using adaptive time series compensator and compliance springs," *Earthquake Eng. Struct. Dyn.*, vol. 47, no. 4, pp. 854–871, 2018.
[11] A. Alleyne and R. Liu, "On the limitations of force tracking control for hydraulic servosystems," *J. Dyn. Syst., Meas., Control*, vol. 121, no. 2, pp. 184–190, 1999.
[12] N. Niksefat and N. Sepehri, "Designing robust force control of hydraulic actuators despite system and environmental uncertainties," *IEEE Control Syst.*, vol. 21, no. 2, pp. 66–77, Apr. 2001.
[13] D. T. Liem, D. Q. Truong, H. G. Park, and K. K. Ahn, "A feedforward neural network fuzzy grey predictor-based controller for force control of an electro-hydraulic actuator," *Int. J. Precis. Eng. Manuf.*, vol. 17, no. 3, pp. 309–321, Mar. 2016.
[14] S. He, "Neural predictive force control for a hydraulic actuator: Simulation and experiment," *Appl. Artif. Intell.*, vol. 23, no. 2, pp. 151–167, 2009.
[15] J. Pan, G. L. Shi, and X. M. Zhu, "Force tracking control for an electro-hydraulic actuator based on an intelligent feed forward compensator," *Proc. Inst. Mech. Eng. C, J. Eng. Mech. Eng. Sci.*, vol. 224, no. C4, pp. 837–849, 2010.
[16] M. Jerouane, N. Sepehri, and F. Lamnabhi-Lagarrigue, "Dynamic analysis of variable structure force control of hydraulic actuators via the reaching law approach," *Int. J. Control*, vol. 77, no. 14, pp. 1260–1268, 2004.
[17] L. Xiao, B. Lu, B. Yu, and Z. Ye, "Cascaded sliding mode force control for a single-rod electrohydraulic actuator," *Neurocomputing*, vol. 156, pp. 117–120, May 2015.
[18] X. Zhu, H. Zhang, B. Yang, and G. Zhang, "Cloud-based shaft torque estimation for electric vehicle equipped with integrated motor-transmission system," *Mech. Syst. Signal Process.*, vol. 99, pp. 647–660, Jan. 2017.
[19] X. Zhu, F. Meng, H. Zhang, and Y. Cui, "Robust driveshaft torque observer design for stepped ratio transmission in electric vehicles," *Neurocomputing*, vol. 164, pp. 262–271, Sep. 2015.
[20] H. Zhang and J. Wang, "State estimation of discrete-time Takagi–Sugeno fuzzy systems in a network environment," *IEEE Trans. Cybern.*, vol. 45, no. 8, pp. 1525–1536, Aug. 2015.
[21] S.-L. Shi, J.-X. Li, and Y.-M. Fang, "Extended-state-observer-based chattering free sliding mode control for nonlinear systems with mismatched disturbance," *IEEE Access*, vol. 6, pp. 22952–22957, 2018.
[22] A. Levant, "Higher-order sliding modes, differentiation and output-feedback control," *Int. J. Control*, vol. 76, nos. 9–10, pp. 924–941, Jan. 2003.
[23] G. Palli, S. Strano, and M. Terzo, "Sliding-mode observers for state and disturbance estimation in electro-hydraulic systems," *Control Eng. Pract.*, vol. 74, pp. 58–70, May 2018.
[24] C. Wang, M. Liang, and C.-N. Li, "Adaptive fuzzy sliding mode observer for cylinder mass flow estimation in SI engines," *IEEE Access*, vol. 6, pp. 29558–29566, 2018.
[25] H. Sun and G. T.-C. Chiu, "Nonlinear observer based force control of electro-hydraulic actuators," in *Proc. Amer. Control Conf.*, San Diego, CA, USA, 1999, pp. 764–768.
[26] P. Nakkarat and S. Kuntanapreeda, "Observer-based backstepping force control of an electrohydraulic actuator," *Control Eng. Pract.*, vol. 17, no. 8, pp. 895–902, 2009.

[27] X. Wang, X. Sun, S. Li, and H. Ye, "Output feedback domination approach for finite-time force control of an electrohydraulic actuator," *IET Control Theory Appl.*, vol. 6, no. 7, pp. 921–934, May 2012.
[28] D. Won, W. Kim, and M. Tomizuka, "High-gain-observer-based integral sliding mode control for position tracking of electrohydraulic servo systems," *IEEE/ASME Trans. Mechatronics*, vol. 22, no. 6, pp. 2695–2704, Dec. 2017.
[29] W. Kim, D. Won, and C. C. Chung, "High gain observer based nonlinear position control for electro-hydraulic servo systems," in *Proc. Amer. Control Conf. (ACC)*, Baltimore, MD, USA, 2010, pp. 1440–1446.
[30] W. Kim, D. Won, D. Shin, and C. C. Chung, "Output feedback nonlinear control for electro-hydraulic systems," *Mechatronics*, vol. 22, no. 6, pp. 766–777, 2012.
[31] A. Šabanovic, "Variable structure systems with sliding modes in motion control—A survey," *IEEE Trans. Ind. Informat.*, vol. 7, no. 2, pp. 212–223, May 2011.
[32] C. Guan and S. Pan, "Adaptive sliding mode control of electro-hydraulic system with nonlinear unknown parameters," *Control Eng. Pract.*, vol. 16, no. 11, pp. 1275–1284, 2008.
[33] B. Yao, F. Bu, J. Reedy, and G. T.-C. Chiu, "Adaptive robust motion control of single-rod hydraulic actuators: Theory and experiments," *IEEE/ASME Trans. Mechatronics*, vol. 5, no. 1, pp. 79–91, Mar. 2000.
[34] H. E. Merritt, *Hydraulic Control Systems*. New York, NY, USA: Wiley, 1967.
[35] Robert Bosch GmbH, *Electrohydraulic Proportional and Control Systems*. Ditzingen, Germany: Omegon, 1999.
[36] M. Farza, M. M'Saad, and L. Rossignol, "Observer design for a class of MIMO nonlinear systems," *Automatica*, vol. 40, no. 1, pp. 135–143, 2004.
[37] M. Farza, M. M'Saad, and M. Sekher, "A set of observers for a class of nonlinear systems," *IFAC Proc. Volumes*, vol. 38, no. 1, pp. 765–770, 2005.
[38] A. Ayadi, S. Hajji, M. Smaoui, A. Chaari, and M. Farza, "A high gain observer coupled to a sliding mode technique for electropneumatic system control," in *Proc. STA-Int. Conf. Sci. Tech. Autom. Control Comput. Eng.*, Hammamet, Tunisia, 2014, pp. 963–967.
[39] A. Ayadi, S. Hajji, M. Smaoui, A. Chaari, and M. Farza, "Experimental sensorless control for electropneumatic system based on high gain observer and adaptive sliding mode control," *Int. J. Adv. Manuf. Technol.*, vol. 93, nos. 9–12, pp. 4075–4088, 2017.
[40] D. Q. Zhang and S. K. Panda, "Chattering-free and fast-response sliding mode controller," *IEE Proc.-Control Theory Appl.*, vol. 146, no. 2, pp. 171–177, Mar. 1999.
[41] A. N. Atassi and H. K. Khalil, "A separation principle for the stabilization of a class of nonlinear systems," *IEEE Trans. Autom. Control*, vol. 44, no. 9, pp. 1672–1687, Sep. 1999.
[42] H. K. Khalil, "High-gain observers in nonlinear feedback control," in *Proc. Int. Conf. Control., Autom. Syst. (ICCAS)*, Seoul, South Korea, 2008, pp. 13–23.
[43] K. K. Young, P. Kokotović, and V. Utkin, "A singular perturbation analysis of high-gain feedback systems," *IEEE Trans. Autom. Control*, vol. AC-22, no. 6, pp. 931–938, Dec. 1977.

GUOSHENG XU received the B.S. degree from Shandong Agricultural University, Tai'an, China, and the M.S. degree from Guizhou University, Guiyang, China, all in mechatronic engineering. He is currently pursuing the Ph.D. degree with the Harbin Institute of Technology, Harbin, China.

His research interest includes the automation of the hydraulic excavator.

NIANLI LU received the B.S. degree from the Xi'an University of Architecture and Technology, Xi'an, China, in 1978, the M.S. degree from the Harbin Institute of Technology, Harbin, China, in 1981, and the Ph.D. degree from Technischen Universität Darmstadt, Darmstadt, Germany, in 1988.

As a Professor and a Doctoral Tutor of the Harbin Institute of Technology, he was involved in the areas of structural mechanics and dynamics analysis of the mechanical systems.

GUANGMING LV received the B.S., M.S., and Ph.D. degrees from the Harbin Institute of Technology, Harbin, China, in 1985, 1988, and 2008, respectively.

He is currently a Professor with the Harbin Institute of Technology and has worked in the areas of the automation of the engineering machinery and the robotic systems.